Nanotechnology, Science and Applications

Dovepress
Taylor & Francis Group

Open Access Full Text Article

ORIGINAL RESEARCH

Polymer-Lipid Hybrid Nanoparticles for Enhanced Gentamicin Efficacy Against Drug-Resistant Bacteria

Alaa Eldeen Yassin[1,2], Faisal Alsuwayyid[1,3], Lama Alkhathran[1], Sabiha Alrouisan[1], Ghadah Alotaibi[1], Majd Alyaqub[1], Weam Alsalman[1], Raghad R Alzahrani[2,4], Ibrahim Farh[1,2], Majed Halwani[1,2], Shmeylan Al Harbi[1,2,5]

[1]Department of Pharmaceutical Sciences, College of Pharmacy, King Saud bin Abdulaziz University for Health Sciences, Riyadh, 11481, Saudi Arabia; [2]Nanomedicine Department, King Abdullah International Medical Research Center, Riyadh, 11481, Saudi Arabia; [3]Department of Industrial and Molecular Pharmaceutics, Purdue University, West Lafayette, IN, 47907, USA; [4]Department of Botany and Microbiology, College of Science, King Saud University, Riyadh, 11451, Saudi Arabia; [5]Pharmaceutical Care Department, King Abdulaziz Medical City, National Guard Health Affairs, Riyadh, 11426, Saudi Arabia

Correspondence: Alaa Eldeen Yassin, College of Pharmacy, King Saud bin Abdulaziz University for Health Science, P.O. Box 3660, Riyadh, 11481, Saudi Arabia, Tel +966114295038, Email yassina@ksau-hs.edu.sa

Nanotechnology, Science and Applications downloaded from https://www.dovepress.com/
For personal use only.

Purpose: Antibiotic resistance is a critical global health concern, exacerbated by biofilm formation and the declining effectiveness of conventional therapies. This study investigates polymer-lipid hybrid nanoparticles (PLNs) as an innovative nanocarrier system to enhance the antibacterial efficacy of gentamicin (Gen) while overcoming its inherent hydrophilicity and poor encapsulation efficiency.

Methods: Using an optimized double-emulsification/solvent-evaporation technique, PLNs were designed to improve drug encapsulation efficiency (EE%) and loading capacity (DL%). The resulting formulations (F0, f1, F2, F3, F4) were characterized for particle size, polydispersity index (PDI), zeta potential, and EE%. Transmitted electron microscopy (TEM) provided insights into particle morphology, while antibacterial activity was tested against multiple bacterial strains, including resistant isolates.

Results: The optimized formulation (F4) demonstrated favorable characteristics ($p \leq 0.05$) including, EE% of 42.1±3.8%, a DL% of 8.0±0.7%, and uniform small average particle size (143.4±3.69 nm) and zeta potential −37.9±3.1 mV. TEM analysis confirmed Gen encapsulation within the lipid-polymer matrix. In vitro antibacterial assays demonstrated that F4 significantly enhanced antibacterial activity ($p \leq 0.05$), achieving up to a 160-fold reduction in minimum inhibitory and bactericidal concentrations (MIC/MBC) against Methicillin-resistant *Staphylococcus aureus* (MRSA-59) and *Pseudomonas aeruginosa* (PA-78) compared with free Gen.

Conclusion: These findings underscore the potential of PLNs as a robust platform for targeted drug delivery, offering a promising strategy to combat antimicrobial resistance.

Keywords: polymer-lipid hybrid nanoparticles, gentamicin, double-emulsification/solvent-evaporation, entrapment efficiency

Introduction

Antibiotic resistance is a major global concern worldwide.[1,2] Over 500,000 infections were caused by antibiotic-resistant bacteria resulting in more than 30,000 deaths in 2015 in Europe alone as The European Centre for Disease Prevention and Control reported.[3] According to the US Centers for Disease Control and Prevention (CDC), at least 23,000 people in the US die from antibiotic-resistant diseases each year, which impact over two million people annually.[4] As the effect of antibiotics are diminished, infections such as tuberculosis, pneumonia, and gonorrhea are becoming challenging and even impossible to treat.[1,5–7]

One of the strategies used by bacteria resistant to antibiotics is the production of bio-films.[3,8] The term "biofilm" first mentioned in a publication authored by Costerton et al.[9] Later, they defined it as an ordered population of microorganisms that are clinging to a surface and are enclosed in a framework of polymers that the bacteria produces.[10] Chronic infections caused by biofilm-forming bacteria are characterized by persistent tis-sue damage and inflammation that

Received: 23 June 2025
Accepted: 2 December 2025
Published: 9 December 2025

© 2025 Yassin et al. This work is published and licensed by Dove Medical Press Limited. The full terms of this license are available at https://www.dovepress.com/terms.php and incorporate the Creative Commons Attribution – Non Commercial (unported, v4.0) License (http://creativecommons.org/licenses/by-nc/4.0/). By accessing the work you hereby accept the Terms. Non-commercial uses of the work are permitted without any further permission from Dove Medical Press Limited, provided the work is properly attributed. For permission for commercial use of this work, please see paragraphs 4.2 and 5 of our Terms (https://www.dovepress.com/terms.php).

persists even after multiple antibiotic treatments.[11] Furthermore, mutations, horizontal gene transmission, and anaerobic conditions inside biofilms all contribute to the reduction of antibiotic susceptibility in biofilms.[11,12]

Aminoglycosides (AGs) are broad-spectrum antibiotics with bactericidal activity that were among the first to be identified and used in clinical practice.[13] They are mostly used to treat infections brought on by aerobic gram-negative organisms such *Serratia spp.*, *Klebsiella pneumoniae*, and *E coli*.[13,14] They function by blocking the bacterial ribosome's 30S subunit from attaching to messenger RNA, which inhibits the synthesis of proteins.[15] They are frequently used as first-line therapy for diseases like meningitis, endocarditis, and some respiratory infections.[14] However, their clinical use has been limited due to their established toxicities that includes nephrotoxicity, irreversible ototoxicity, and neuromuscular blockade.[16–18]

Antimicrobial resistance to AGs is becoming an escalating global health concern, particularly as AGs are frequently used as last-line treatments for severe infections like multidrug-resistant tuberculosis (MDR-TB) and MRSA.[19] Gen, a commonly used AG, is increasingly hindered by bacterial resistance mechanisms. Resistance can develop through changes in the antibiotic's target, efflux mechanisms, or enzymatic modifications.[20] The most common resistance mechanism involves chemical modification by amino-glycoside-modifying enzymes, which fall into three main categories: acetyltransferases, nucleotidyl transferases, and phosphotransferases.[21] Additional resistance mechanisms include mutations in the 16S rRNA gene, which alter the 30S ribosomal subunit target, methylation of the aminoglycoside-binding site, and a reduction in intracellular amino-glycoside concentrations. This reduction is caused by changes in outer membrane permeability, decreased transport across the inner membrane, and active efflux processes.[22] Horizontal gene transfer further facilitates the spread of these resistance mechanisms, enabling resistant traits to propagate within bacterial populations.

Due to their extremely small size, high surface area-to-volume ratio, and capacity to permeate biological fluids and membranes, nanoparticles (NPs) possess special qualities as drug delivery systems.[23,24] They often increase the duration of drug circulation in the body, increase bioavailability, reduce toxicity, and circumvent the difficulties encountered by traditional administration methods since they are larger than the cut-off size of nephrons.[24,25]

Solid lipid nanoparticles (SLNs) are nanoparticulate system made entirely from lipids with melting points higher than common environmental and biological temperatures.[26] Among their many benefits are biocompatibility, protection from harsh environmental conditions, and ease of large-scale synthesis using high-pressure homogenization.[27,28] However, SLNs have drawbacks, including a non-uniform biphasic drug release profile with a high burst effect due to their perfect crystalline structure, which can cause drug expulsion during storage and poor drug loading efficiency limited by the drug's solubility in the particles' lipid matrix.[29] Many attempts in the literature showed the success of drug-loaded SLN in enhancing the activity of many anticancer and anti-bacterial drugs.[30–32]

Polymeric nanoparticles are nanoscale drug carriers that are typically made of bio-degradable and biocompatible polymers. They provide more control over drug release, decreased side effects, and improved therapeutic efficacy.[33] Their chemical and physical stability surpasses that of lipid-based nanoparticles, and they offer enhanced stability for drugs, protecting them from degradation by enzymes or environmental factors.[34] Furthermore, their biodegradability nature ensures their safe fate within the body causing no long-term accumulation or toxicity. Polymeric lipid hybrid nanoparticles (PLNs) have been developed to provide advantages over the drawbacks of both lipid and polymeric nanoparticles. The polymer provides better control on drug release while lipids would enhance drug penetration within biological membranes.[35,36] This can result in having nanoparticles with superior biopharmaceutical properties that can be used to achieve the delivery needs of various drugs and drug combinations.[37]

To enhance the delivery and antibacterial activity of Gen, various strategies have been explored. Nanoparticle-based drug delivery systems, including liposomes, solid lipid nanoparticles (SLNs), and polymeric nanoparticles, have been investigated to improve the solubility, stability, and targeted delivery of Gen.[38–40] Notably, negatively charged liposomal formulations have demonstrated a significant increase in Gen's antibacterial activity and biofilm prevention [39]. Polymeric nanoparticles, composed of materials such as poly-lactic-co-glycolic acid (PLGA) and chitosan, have also proven highly effective in enhancing the antibacterial activity of Gen against a wide range of bacterial strains.[39,40]

Formulating Gen into nanoparticles, which often rely on lipophilic or amphiphilic interactions for drug loading, is extremely difficult due to its great hydrophilicity and low log P (partition coefficient). Conventional nanoparticle systems

have demonstrated limited success in overcoming these issues. Polymeric nanoparticles, although offering excellent stability and controlled release, often show poor entrapment of hydrophilic drugs because Gen rapidly diffuses into the aqueous phase during the emulsification process.[39,40] Similarly, lipid-based systems such as solid lipid nanoparticles (SLNs) and liposomes frequently exhibit low encapsulation efficiency and high burst release, primarily due to the weak affinity of hydrophilic molecules for the lipid matrix.[38] Effective drug loading is hampered by the mismatch between Gen's water-loving nature and the typically lipophilic character of many nanoparticle carriers.[41] PLNs integrate the advantages of both polymeric and lipid-based systems, providing a synergistic structure that enhances encapsulation and stability. The polymeric core ensures sustained and controlled drug release, while the surrounding lipid layer improves drug retention, biocompatibility, and interaction with bacterial membranes.[42] This dual-matrix design minimizes drug leakage during preparation and storage and facilitates improved penetration through bacterial and biofilm barriers. Previous studies have also demonstrated that PLNs can enhance the therapeutic performance of antibiotics against resistant pathogens, supporting their selection in this study as an optimized strategy for efficient Gen delivery.[43]

Specifically, we now emphasize that conventional Gen formulations face major limitations such as poor encapsulation efficiency, short duration, and reduced efficacy against resistant bacteria due to efflux pumps and biofilm barriers. This study aims to develop and optimize a PLN system designed to enhance Gen encapsulation, sustain release, and improve antibacterial activity against resistant strains.

Materials and Methods

Materials

Gentamicin, polycaprolactone (PCL, Mw 42,000 Da), polyvinyl alcohol, stearic acid, Span 80 and Tween 80 were purchased from Sigma-Aldrich Chemical Co. (St. Louis, MO, USA) through local distributer in Saudi Arabia. Dynasan 118 were purchased from Sasol Germany GmbH (Witten, Germany). Mueller Hinton Agar was obtained from HiMedia Laboratories Pvt. Ltd. (Mumbai, India).

Bacterial Isolates

All bacterial isolates were collected anonymously following hospital routine procedures and before disposal. The bacterial isolates source was king Abdulaziz medical city of National Guard Health Affairs, Riyadh, Saudi Arabia through the Infectious Diseases Department at King Abdullah International Medical Research Center. ATCC reference strains were obtained from the American Type Culture Collection (ATCC, Manassas, VA, USA). Gram-positive and Gram-negative bacterial identities were confirmed by Gram staining and bacteria susceptibility profiling was obtained by vitek machine before inclusion the isolates in the assays. All Bacterial samples including ATCC strains were sub-cultured at 37°C for 24h by Luria-Bertani (LB) agar. All antibacterial experiments were standardized by following the values of CLSI guidelines.

Methods

Preparation of PLN Drug Formulation

The double-emulsification/solvent-evaporation method described earlier by Omer et al[44] was employed with minor modifications for the co-encapsulation of Gen into an optimized PLN. Briefly, an organic phase was developed by dissolving certain weights of PCL, stearic acid, and Span 80 in 10 mL chloroform. Certain weights of Gen and Tween 80 were dissolved in 2 mL of water as an aqueous phase. PVA solutions (1 or 1.5%) were used as secondary emulsification agent in formulations F2, F3, and F4 while Tween 80 was used in the case of F1. The aqueous phase was emulsified in the organic phase by probe-sonication for 3 min at 60% voltage efficiency under ice bath utilizing Q700; Qsonica LLC, (Newton, CA, USA). The formed primary emulsion was mixed with certain volume of either PVA or Tween 80 solutions and a secondary emulsion was developed using a second probe-sonication cycle for 5 min. The prepared double emulsion was stirred continuously overnight under to ensure complete removal of chloroform for formulations F0, F1, F2, and F3. For formulation F4, chloroform removal was achieved using a rotary evaporator (BUCHI, Flawil, Switzerland), operated at 100 rpm and 40°C for 1 hour to accelerate solvent evaporation. The resulting PLNs were collected by centrifugation at

Table 1 The Composition of the Prepared Formulations (F0, F1, F2, F3, F4)

Formula Code	Drug	Polymer	Lipids		Primary Surfactant and Co-surfactant		Secondary Surfactant	
	Gen	PCL	Dyansan	SA	Tween 80	Span 80	PVA	Tween 80
F0 (Void) *	0	240 mg	25 mg	25 mg	50 mg	50 mg	15 mL (1%)	X
F1	5 mg	150 mg	25 mg	25 mg	25 mg	50 mg	X	30 mL (1%)
F2	5 mg	150 mg	25 mg	25 mg	25 mg	50 mg	40mL (1.5%)	X
F3	40 mg	150 mg	25 mg	25 mg	25 mg	50 mg	40 mL (1%)	X
F4	60 mg	240 mg	25 mg	25 mg	50 mg	50 mg	15 mL (1%)	X

Note: * F0 (void batch) was prepared following the same method as F4 but without drug addition.
Abbreviations: Gen, Gentamicin; PCL, Polycaprolactone; SA, Stearic Acid; PVA, Polyvinyl alcohol.

15,000 relative centrifugal force (RCF) for 30 min, and the pellet was washed twice with distilled water to remove un-encapsulated drug. The purified residue was then redispersed in a minimal volume of distilled water, frozen at −80°C and subsequently lyophilized using a Christ freeze-dryer model Beta 2–8 LD Plus (Martin Christ, Germany). The exact composition and formulation parameters are listed in Table 1. In order to increase the Gen entrapment efficiency (EE) %, number of approaches was employed including reducing the volume of water in the double emulsion, increasing the Gen concentration in the aqueous phase, and minimizing the chloroform evaporation time to only one hour by using the rotary evaporator Figure 1 represents a detailed diagram for the finally optimized method.

Evaluation of the Physical Characteristics of the Prepared PLN

Determination of Particle Size and Polydispersity Index

The particle size and polydispersity of all the formed PLN were measured after dilution with distilled water to almost 0.1% w/v concentration of nanoparticles dispersion utilizing a Brookhaven ZetaPALS (Brookhaven Instruments Corporation, Holtsville, NY, USA). A 90° angle was adjusted for all measurements.

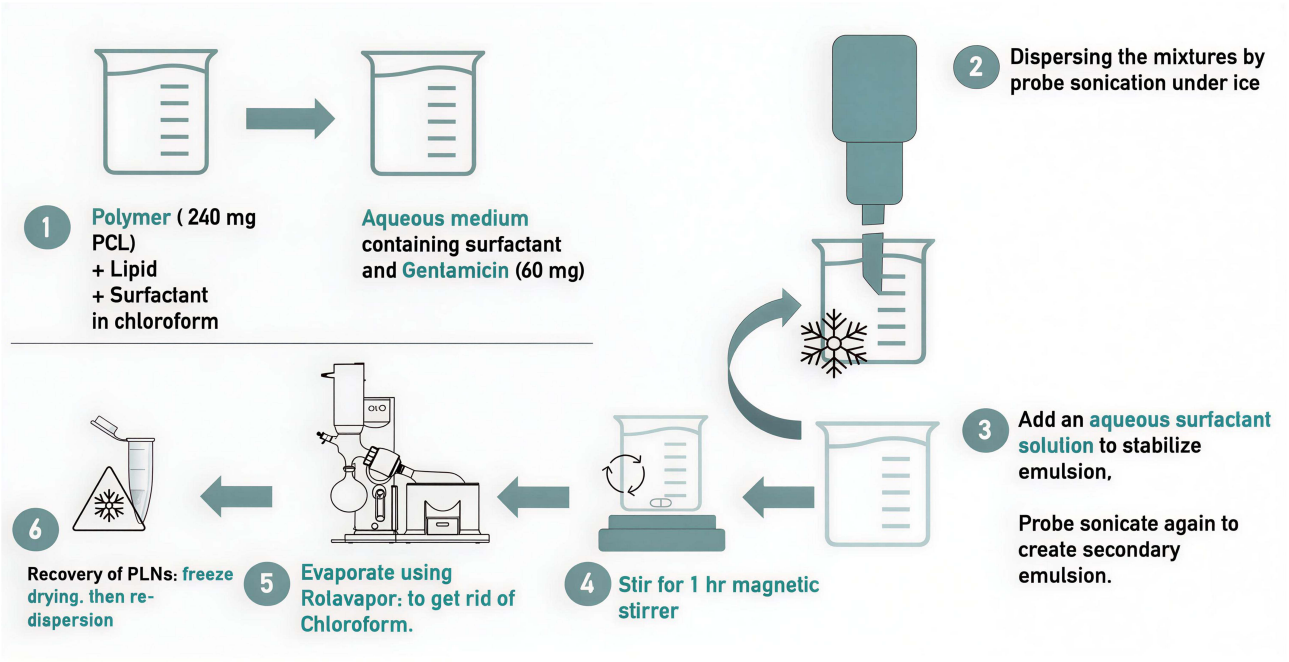

Figure 1 The double-emulsification/solvent-evaporation method diagram.

Determination of Zeta-Potential

ZetaPALS was also employed for zeta potential measurement for all the diluted samples used for particle size measurement applying the mode of the laser Doppler velocimetry.

Particle Morphological Features

A sample from the freeze-dried PLN was weighed and dispersed in distilled water to give 1 mg/L dispersion. The dispersions were sonicated for 10 min in Ultrasonic bath solicitor to render their original particle sizes. Then, one droplet of each dispersion was placed onto a carbon-coated copper grid of 400-mesh and allowed to dry at room temperature. Particle morphology and composition were inspected using a JEM-1400 transmitted electron microscopy [TEM], (JEOL, Tokyo, Japan) at acceleration voltage of 120 KV.

Drug Loading (DL%) and Entrapment Efficiency (EE)%

Both EE% and DL% were calculated indirectly based on the amount of unentrapped Gen determined in the supernatant of the centrifuged nano-dispersion. Gen was determined by a simple spectrophotometric method. Simply, a set of Gen standard solutions in distilled water was prepared by in concentration range from 25 to 100 μg/mL. A standard calibration curve was constructed after measuring the UV absorbance at λmax = 255 nm utilizing a Thermo Fisher Scientific Evolution 60S UV/Visible Spectrophotometer (Waltham, Massachusetts, United States). The standard curve showed high linearity in this concentration range with R^2 value = 0.9983. The method was validated by repeating the standard curve at 3 different times within the same day (intra-day) and at three different days (inter-day). The EE% and DL% for each formulation were calculated using the following equations:

$$EE\% = \frac{\text{initial drug weight} - \text{unentrapped free drug}}{\text{initial drug weight}} \times 100 \quad (1)$$

$$DL\% = \frac{\text{initial drug weight} - \text{unentrapped free drug}}{\text{total weight of PLN}} \times 100 \quad (2)$$

Physical Stability of the Prepared PLN Formulations

PLN dispersion 1% in distilled water from F4 was stored in refrigerator for 25 days. Samples were taken periodically and the particle size and PDI were determined for each sample.

Evaluation of the Antibacterial Activity

Tested Bacteria and Growth Conditions

A diverse panel of bacterial strains was evaluated, including both ATCC reference strains and clinical isolates, representing Gram-positive and Gram-negative species. Bacteria were initially revived from glycerol stocks stored at –40°C by streaking onto Luria-Bertani (LB) agar plates, followed by incubation at 37°C for 18–20 hours to obtain fresh cultures. For the minimum inhibitory concentration (MIC) assays, pathogens were cultured in Mueller-Hinton Broth (MHB). The minimum bactericidal concentration (MBC) was subsequently determined by plating on Mueller-Hinton Agar (MHA) and incubating at 37°C for 18–20 hours. All experimental incubations were performed under these standardized conditions.[45]

Antibacterial Assays

Minimum Inhibitory Concentration (MIC)

The MIC was determined using a 96-well microliter plate according to the 2003 EUCAST/ESCMID guidelines, with minor modifications.[46] Briefly, 100 μL of Mueller-Hinton Broth (MHB) was added to each well. Two-fold serial dilutions of the Gen Formula were prepared by transferring 100 μL of the formula into successive wells. The concentration range for the Gen Formula was 12.5 to 0.39 μg/mL, while free Gen was tested at concentrations from 32 to 1 μg/mL. The bacterial inoculum was standardized to a 0.5 McFarland turbidity using 0.9% saline and then diluted in MHB to achieve a final concentration of 5×10^5 CFU/mL in each well. MHB alone served as the sterility control (negative control), and

MHB with bacterial suspension served as the growth control (positive control). Plates were incubated in a rotary shaker at 90 rpm.

Minimum Bactericidal Concentration (MBC)

After 18–20 hours of incubation, a loopful (1 µL) from each test well was streaked onto Mueller-Hinton Agar (MHA) plates. These plates were incubated for an additional 18–20 hours at 37°C. The MBC was defined as the lowest concentration resulting in ≥99% bacterial inhibition.

Results

Formulations and Method Development

Table 1 shows the exact modifications and difference between the four formulations. Four PLN formulations were prepared varying a number of factors including; drug to PCL ratio, lipids to PCL ratio, the secondary surfactant type and volume, and the amount of Tween 80. The variation in those factors was attempted to improve the EE% of Gen and the characteristics of the produced NPs. The double emulsification–solvent evaporation method was employed in the preparation of PLN. In formulation 4, rota-evaporator was used to shorten the time of chloroform removal as well as the volume of the aqueous phase was tremendously reduced in order to minimize the escape of Gen into the aqueous phase and subsequently increase the EE%. Figure 1 represents a diagram illustrating the method employed for PLN preparation.

Polymer-Lipid Hybrid Nanoparticle Characterization

All formulations displayed nanoparticle sizes ranging from 143.4 to 339.9 nm, with polydispersity (PDI) indices between 0.18 and 0.9 as shown in Table 2 and Figure 2. The particle size was influenced by the type and concentration of the secondary surfactant. Both F3 and F4, which were formulated with 1% PVA as the secondary surfactant, showed particle sizes of 251.5 nm and 143.4 nm, respectively. These sizes were notably smaller compared to F1 and F2. When the concentration of Tween 80 was doubled to equalize Span 80 and the volume of PVA was reduced from 40 mL (as in F3) to 15 mL (as in F4), a significant decrease in particle size ($p \leq 0.05$) was observed. In contrast, using 1% Tween 80 as the secondary surfactant (in F1) led to a higher PDI of 0.9. However, all formulations containing PVA demonstrated excellent particle size uniformity, as indicated by PDI values ≤ 0.25. This is also clear from the size distribution curves represented in Figure 2C and D where they display single narrow peaks indicating high uniformity in particle sizes.

Zeta Potential

Table 2 illustrates the zeta potential values for the four formulations. All formulations displayed similar values around −38 mV, except for F3, which had a zeta potential of −11.94 mV. The high zeta potential in the other formulations indicates strong particle stability and resistance to aggregation. In contrast, the lower value for F3 suggests it may be more susceptible to aggregation, potentially resulting in a shorter shelf life and diminished performance.

Table 2 Characteristics of the Four Formulations Prepared in the Study

Formulation	Drug:Polymer Ratio	Mean Particle Size (nm) (Mean ± SD)	PDI	Zeta Potential (mV)	EE %	DL%
F0 (Void)	–	178. ± 4.5	0.34± 0.02	–		
F1	1:30	317.43 ±11.85	0.9± 0.06	− 38.0± 4.3	1.7± 0.6%	0.04± 0.01%
F2	1:30	339.98± 3.81	0.18± 0.01	− 38.1± 5.0	2.4± 0.8%	0.06± 0.02%
F3	1:3.75	251.56± 3.1	0.21±0.01	−11.9± 2.6	4.8± 1.1%	0.95± 0.23%
F4	1:4	143.42± 3.69	0.25± 0.01	− 37.9± 3.1	42.1± 3.8%	8.01± 0.73%

Abbreviations: PDI, Polydispersity index; EE%, Entrapment efficiency percent; DL%, Drug loading percent.

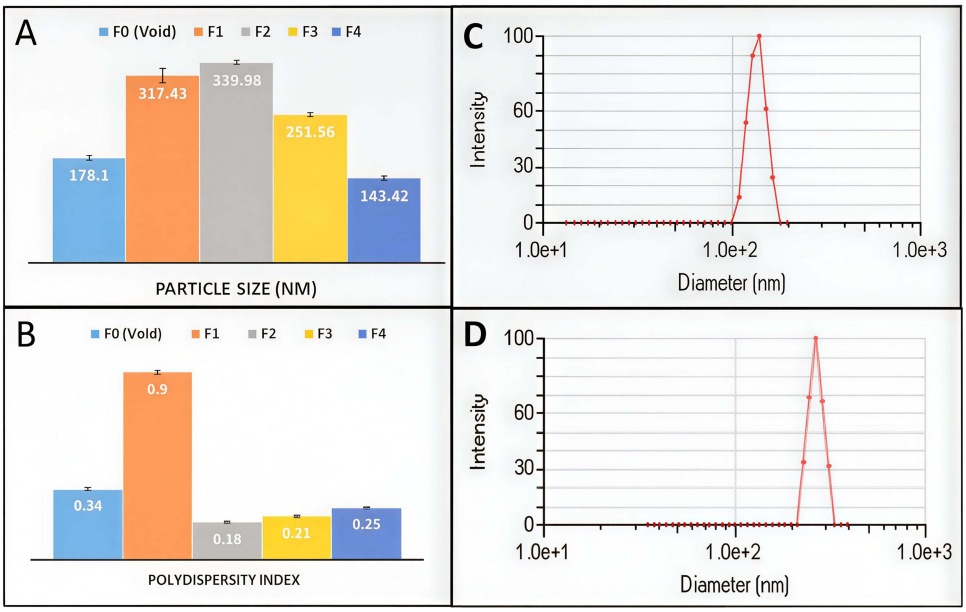

Figure 2 The mean of particle size and polydispersity index (PDI) for all PLN formulations.
Notes: (**A**) The mean ± standard deviation in nm of the particle size for all formulations, (**B**) The mean ± standard deviation of the polydispersity index (PDI) for all formulations, (**C**) DLS spectrum showing light scattering intensity percentages of F4, (**D**) DLS spectrum showing light scattering intensity percentages of F3. Each experiment was conducted in triplicate (n = 3).

Drug Loading (DL%) and Entrapment Efficiency (EE%)

The encapsulation efficiency (EE%) in F1 was found to be very low, at only 1.7%, presenting a significant challenge. Replacing Tween 80 with 1.5% PVA as the stabilizer in F2 did not result in a noticeable improvement in EE%. Reducing the PVA concentration to 1% and increasing the amount of Gen (40 mg) while lowering the drug-to-PCL ratio in F3 led to a slight increase in EE% to 4.7%, but this was still considered very low. However, by minimizing the water volume in both the primary and secondary emulsions and shortening the time for chloroform removal using a rotary evaporator, a substantial improvement in EE% was observed in F4, reaching 42%. In terms of drug loading (DL%), values were below 1% for all formulations except F4, which had a DL% of 7.2%.

Morphological Analysis

The results presented in Figure 3 provide insightful details regarding the morphology and structure of F4 PLN (lipid-polymer conjugate particles) across different magnification levels. Image A offers a broad overview of the particle distribution, revealing a dense population of particles with relatively uniform sizes. This size range is notably smaller than those observed through light scattering techniques, which likely highlights the superior resolution and sensitivity of the imaging method employed. The particles exhibit spherical to slightly oval shapes, typical for lipid-polymer conjugate particles. Images B, C, and D provide more detailed views of selected particles, showing variations in black and white intensity. The presence of varying black and white intensities within the particles suggests the potential for heterogeneous internal distribution of components. These intensity differences highlight multiple dark spots in the particles' cores, suggesting the encapsulation of Gen within the particle matrices.

Physical Stability of PLN

As shown in Figure 4A, the particle size of formulation F4 increased from approximately 143 nm at day 0 to around 360 nm by day 6, followed by a slight reduction to ~308 nm after 25 days of storage. This initial increase in size may be attributed to particle swelling or limited aggregation due to water diffusion into the polymer matrix. The subsequent reduction in size indicates that the system reached a more thermodynamically stable equilibrium.

In parallel, the PDI (Figure 4B) decreased steadily from 0.18 to 0.09 over the 25-day storage period, suggesting improved particle uniformity and monodispersity. This trend demonstrates that the formulation maintained high colloidal

https://doi.org/10.2147/NSA.S548941

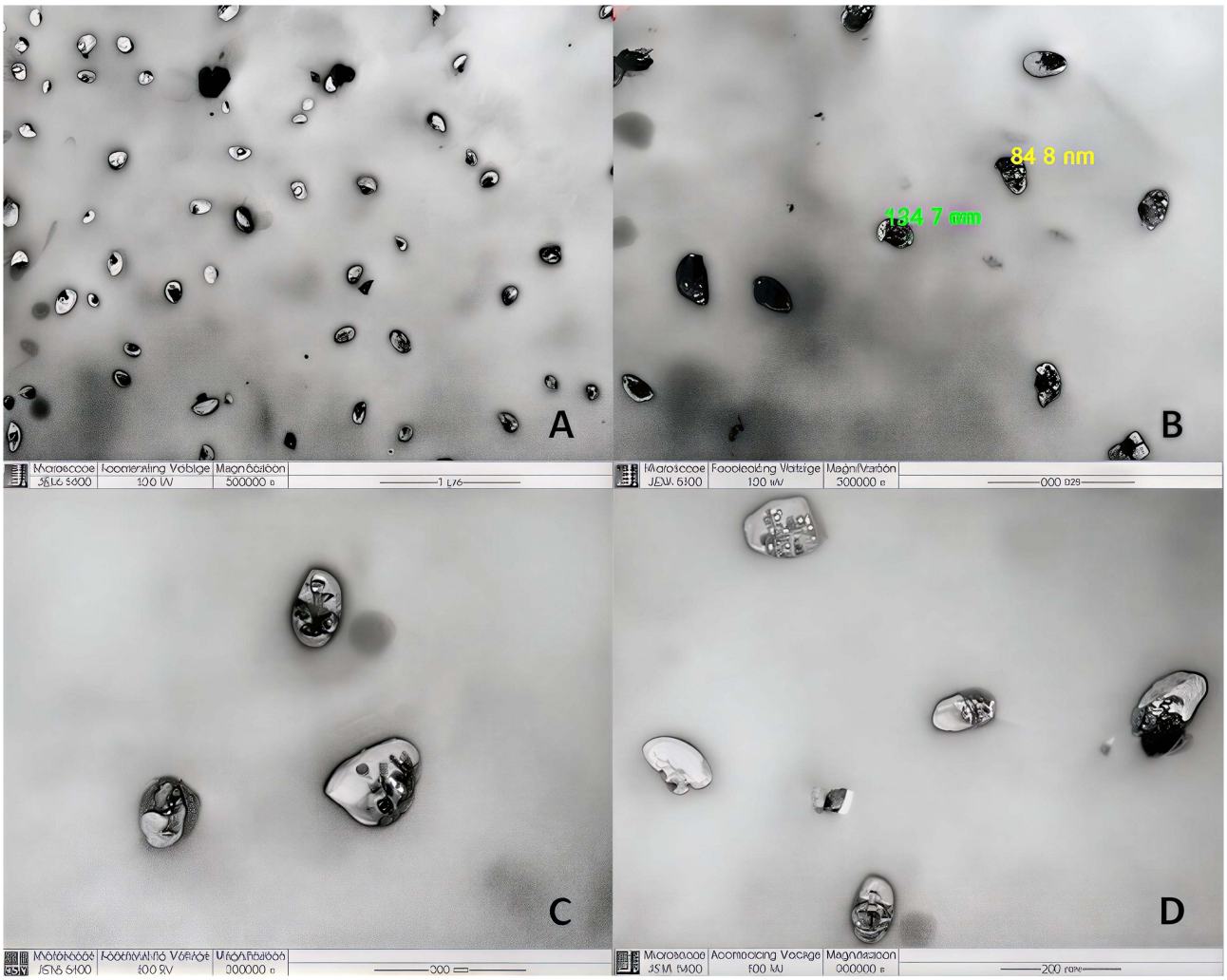

Figure 3 TEM Micrographs of the Gentamicin-Loaded PLN Formulation (F4).
Notes: (**A**) Wide field view showing a high density of particles. (**B**) Closer view with particle diameter measurements. (**C** and **D**) Higher magnification focusing on individual particles.

stability, likely due to the strong negative zeta potential (−37.9 mV), which provided effective electrostatic repulsion and prevented irreversible aggregation. The results demonstrate minimal changes in particle size, PDI, and zeta potential parameters (<10%), confirming the physical stability and homogeneity of the nanoparticles under both refrigerated and ambient conditions. Overall, these results confirm that the optimized PLN (F4) formulation retained good physical stability throughout the storage period.

Antimicrobial Analysis

The antibacterial activity of the optimized PLN formulation, F4, was evaluated by comparing its MIC and MBC values to those of pure Gen at equivalent concentrations against seven bacterial strains, including two ATCC strains and five clinical isolates, two of which were resistant to Gen. The results, summarized in Table 3, highlight the enhanced efficacy of the F4 formulation. Notably, F4 reduced the MIC of Methicillin-resistant S. aureus (MRSA-59), a resistant clinical isolate, by more than 80-fold (3.125 mg/L) com-pared to free Gen (256 mg/mL), while the MBC was reduced by over 160-fold. Against the clinical isolate *Pseudomonas aeruginosa* (PA-78), F4 significantly lowered both MIC and MBC values by more than four-fold. Similarly, for the resistant clinical isolate E. coli (EC-219), F4 achieved a more than two-

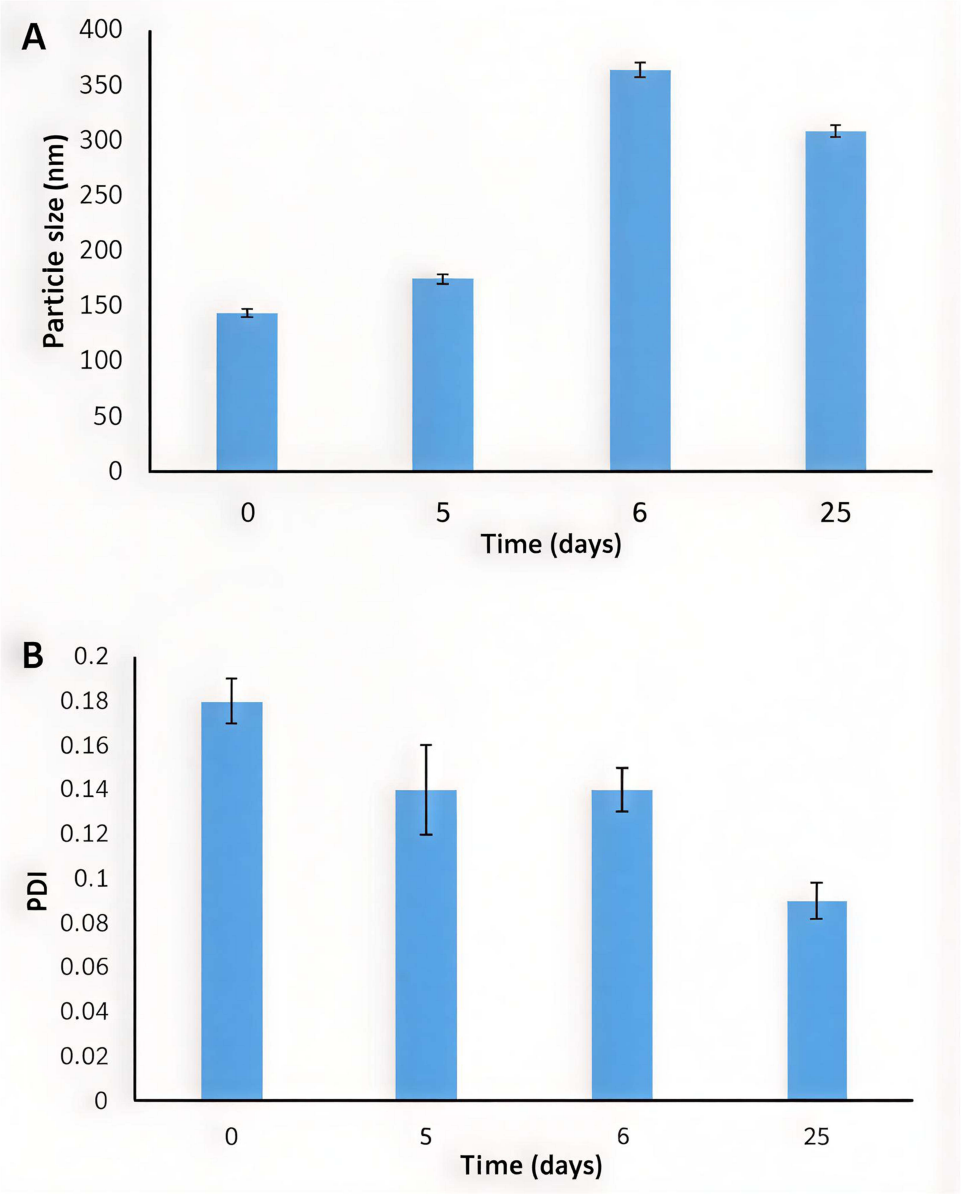

Figure 4 Physical stability of PLN F4 aqueous dispersion for 25 days.
Notes: (**A**) Change in particle sizes, (**B**) change in PDI. Each value represents the mean ± standard deviation (n = 3).

fold reduction in both MIC and MBC values. However, for E. coli ATCC-25922, MRSA-60, and EC-157 strains, no significant reduction in MIC or MBC was observed with the F4 formulation compared to free Gen. These results underscore the potential of F4 in enhancing antibacterial activity, particularly against resistant strains.

Table 3 Antibacterial Activity of Gentamicin-Loaded Polymer–Lipid Hybrid Nanoparticles (F4) Formulation (F4)

No.	Bacteria	AST Profile	Free GEN (mg/L)		F4 Formula (mg/L)	
			MIC	MBC	MIC	MBC
1	*Staphylococcus aureus* ATCC 29213	Susceptible	2	4	0.78	1.56
2	Methicillin-resistant *S. aureus* MRSA-59	Resistant	256	512	3.125	3.125

(*Continued*)

https://doi.org/10.2147/NSA.S548941

Table 3 (Continued).

No.	Bacteria	AST Profile	Free GEN (mg/L)		F4 Formula (mg/L)	
			MIC	MBC	MIC	MBC
3	MRSA-60	Susceptible	2	4	1.56	3.125
4	*Escherichia coli* ATCC 25922	Susceptible	2	4	1.56	3.125
5	*E. coli* EC-157	Susceptible	2	4	1.56	3.125
6	*E. coli* EC-219	Resistant	8	16	3.125	6.25
7	*Pseudomonas aeruginosa* PA-78	Susceptible	8	16	1.56	3.125

Notes: AST profile: Antibiotic susceptibility Test, which are recorded according to The European Committee on Antimicrobial Susceptibility Testing. Breakpoint tables for interpretation of MICs and zone diameters. Version 13.0, 2023. http://www.eucast.org, Access Date: 20 November 2023.
Abbreviations: Gen, gentamicin; MIC, minimum inhibitory concentration; MBC, minimum bactericidal concentration.

Discussion

The observed nanoparticle sizes and PDIs align with the trend reported in the literature, where surfactant selection and concentration play crucial roles in determining the final characteristics of nanoparticles. In particular, particle size and distribution can be significantly influenced by the choice of surfactants used during the formulation process, as well as their concentration.[47] PVA and Tween 80 were chosen for their complementary stabilizing roles and compatibility with polymer–lipid hybrid nanoparticles. Specifically, PVA served as a secondary emulsifier to reduce interfacial tension, prevent aggregation, and ensure steric stability, with low concentrations (≤1%) shown to produce smaller, more uniform nanoparticles by minimizing coalescence during emulsification.[48,49] Moreover, Tween 80 enhances the encapsulation of hydrophilic drugs by reducing drug leakage from the internal aqueous phase, as previously demonstrated in similar polymer–lipid hybrid systems.[44,50] One of the key findings in this study is the impact of the secondary surfactant on particle size. Specifically, formulations containing PVA as a secondary surfactant, such as F2, F3 and F4, displayed smaller PDIs and particle sizes. Reducing the concentration of PVA to 1%, as in F3 and F4, resulted in significant reduction in particle sizes ($p \leq 0.05$) compared with F2 prepared using 1.5% PVA. This result is consistent with findings from several studies that suggest higher concentrations of PVA can increase the viscosity of the formulation, thereby hindering the dispersion of nanoparticles and leading to larger sizes.[48,49] On the other hand, the formulation using 1% Tween 80 as a secondary surfactant (F1) exhibited the largest particle size and the highest PDI. This is in line with literature that suggests that Tween 80, while effective at stabilizing nanoparticles, can result in a broader size distribution at higher concentrations.[51,52] The higher PDI observed in F1 indicates greater heterogeneity in the nanoparticle size distribution, which is typically a result of insufficient stabilization or aggregation during formulation. The results regarding particle size uniformity are promising, as all formulations containing PVA (ie, F3 and F4) displayed excellent particle size uniformity, as indicated by PDI values ≤ 0.25. This finding aligns with the literature, where PVA is frequently employed as a stabilizer due to its excellent ability to reduce particle aggregation and enhance dispersion, resulting in narrower size distributions.[53,54]

Particle size emerges as a pivotal factor influencing both the nanoparticles' systemic circulation longevity and their capacity for passive accumulation within tissues.[55] Previous studies have highlighted the substantial advantages of nanoparticles falling within the size range of approximately 150 nm for effective systemic drug delivery.[55,56] Our optimum formulation, F4, showed particle size close to this range indicating its superior quality and suitability for Gen delivery.

The zeta potential values presented in Table 2 provide important insights into the physical stability and aggregation resistance of the four formulations. Zeta potential is a critical parameter for understanding the stability of colloidal systems, as it reflects the electrostatic repulsion between particles in suspension. In this case, all the formulations

exhibited zeta potential values close to −38 mV, indicating that they possess a high degree of stability. This high negative charge suggests a significant electrostatic repulsion between particles, which would prevent aggregation and enhance the long-term stability of the formulations. Similar findings have been reported by other studies, where zeta potential values in the range of −30 to −40 mV were associated with increased stability of colloidal dispersions.[57,58]

The lipid composition comprising stearic acid and Dynasan 118 in a 1:1 ratio was optimized to achieve an appropriate balance between structural rigidity and membrane permeability within the lipid shell. This combination ensures mechanical stability of the nanoparticle matrix while maintaining sufficient fluidity to enable controlled drug diffusion and effective interaction with bacterial membranes. Stearic acid contributes to the crystalline and thermal stability of the lipid phase, whereas Dynasan 118 (glyceryl tristearate) enhances matrix compactness and minimizes the initial burst release of gentamicin, in agreement with previously reported findings.[27,59]

This low DL% and EE% are often attributed to the limited solubility of the drug in the carrier, inefficient encapsulation processes, or the rapid diffusion of the drug into the aqueous phase during formulation. Studies have highlighted that achieving a high DL% requires careful optimization of the drug-to-polymer ratio, solvent evaporation time, and stabilizer concentration.[60–62] In this case, the use of lower PVA concentrations in F1 to F3 likely did not provide sufficient stabilization of the nanoparticles, which may have hindered the encapsulation efficiency and subsequently led to a low drug loading. The significant improvement in DL% and EE% observed in F4, can likely be attributed to the optimization of the formulation conditions. Reducing the water volume in both the primary and secondary emulsions, doubling the amount of the primary emulsion stabilizer, Tween 80, and shortening the chloroform removal time may have reduced drug loss during the process and maintained a higher concentration of the drug within the nanoparticles. This result aligns with findings by Liu et al[63] who demonstrated that reducing the volume of the aqueous phase during emulsification can limit the drug's diffusion into the surrounding water, thus improving drug loading. Additionally, the time-efficient chloroform evaporation process is known to aid in the preservation of drug encapsulation by preventing excessive leaching of the drug into the external phase.[61] These adjustments were guided by previous studies and preliminary experiments, which demonstrated more efficient formation of PLNs with higher entrapment efficiency.[64]

The spherical to slightly oval shapes of the particles observed in TEM images supports the notion that these particles are indeed lipid-polymer conjugates, as similar particles have been previously described in the literature for their structural and functional properties.[65,66] These intensity differences are indicative of regions with higher electron density, which may correspond to encapsulated substances or areas of lipid aggregation.[67] The dark spots observed in the cores of the particles are particularly noteworthy, as they imply the encapsulation of Gen within the lipid-polymer matrices. The matrix structure likely contributes to the stability of the encapsulated Gen, as lipid-polymer conjugates are known to offer both protection and controlled release properties.[65] This characteristic is particularly advantageous in the context of drug delivery systems, where the aim is to ensure that the active compound is delivered efficiently to the target site without being prematurely released.

The increase in particle size of the F4 dispersion in water over a 25-day storage period may be explained by water diffusion into the PCL matrix, leading to swelling.[68] Another plausible reason is Ostwald ripening, a process commonly observed in lipid-based nanoparticles, particularly when the particles lack sufficient stabilization.[59] Meanwhile, the gradual reduction in PDI to 0.09 by day 25 reflects the transition of the dispersion into a highly monodisperse state. This enhanced uniformity over time could result from the particles settling into a more homogeneous distribution. Research indicates that stabilizers such as surfactants or polymers play a vital role in promoting particle uniformity by preventing aggregation.[50]

The enhanced antibacterial efficacy of the optimized PCL nanoparticle (PLN) formulation, F4, encapsulating Gen, against various bacterial strains, including antibiotic-resistant isolates, demonstrates the significant potential of nanoparticle-based drug delivery systems in combating resistant infections.

F4 achieved a remarkable reduction in MIC and MBC values against Methicillin-resistant *Staphylococcus aureus* (MRSA-59), with MIC decreasing by over 80-fold and MBC by more than 160-fold compared to free Gen. This improvement can be attributed to the enhanced penetration and sustained release properties of the nanoparticle formulation, which allow higher intracellular antibiotic concentrations and help overcome resistance mechanisms. Similar

findings have been reported for Gen combined with threonine amino acid, which significantly enhanced bactericidal activity against MRSA USA300_FPR3757.[69] Additionally, Gen-loaded chitosan nanoparticles have demonstrated enhanced efficacy against *S. aureus*, further supporting the observed results.[70]

Against *Pseudomonas aeruginosa* (PA-78), F4 reduced both MIC and MBC values by more than four-fold. The resistance of *P. aeruginosa* is often attributed to its robust defense mechanisms, such as efflux pumps and biofilm formation. While biofilm activity was not directly assessed in this study, nanoparticle-based delivery systems have been reported to enhance antibiotic efficacy by improving cellular uptake and penetration into bacterial matrices.[71,72] This may partly explain the observed increase in antibacterial activity. This aligns with the findings of Abdelghany et al[73] who demonstrated that Gen-loaded poly(lactide-co-glycolide) nanoparticles reduced colony-forming units and interleukin-6 levels in a peritoneal murine infection model of *P. aeruginosa*, despite higher MIC and MBC values. Furthermore, co-encapsulation of Gen and ascorbic acid into chitosan nanoparticles has been reported to significantly reduce MIC and MBC against *P. aeruginosa*.[74] Enhanced efficacy of Gen has also been demonstrated with Gen-conjugated gold nanoparticles against multiple bacterial strains.[75,76]

For the resistant clinical isolate *Escherichia coli* (EC-219), F4 achieved more than a two-fold reduction in both MIC and MBC values. This improvement can be attributed to better interaction of the nanoparticles with bacterial membranes and the controlled release of Gen, maintaining therapeutic concentrations over time. A recent study reported that co-encapsulation of Gen with thymoquinone into liposomes significantly reduced MIC and MBC values against resistant *E. coli* strains by four-fold.[77] However, for *E. coli* ATCC-25922, MRSA-60, and EC-157 strains, no marked reduction in MIC or MBC was observed with the F4 formulation compared to free Gen. This indicates that the efficacy of nanoparticle-encapsulated antibiotics may vary depending on specific bacterial characteristics, such as membrane permeability, the presence of resistance genes, or biofilm-forming capabilities. Similar findings were observed with other Gen-nanoparticles, such as calcium carbonate and poly(lactide-co-glycolide), which showed MIC values comparable to pure Gen.[78,79] These results highlight the need for tailored approaches when developing nanoparticle-based therapies to target different bacterial pathogens effectively.

The optimized F4 formulation demonstrated markedly superior performance compared with previously reported Gen-loaded nanocarriers. Jia et al[80] developed Gen-loaded liposomes composed of DPPC and cholesterol, achieving a maximum EE of only 25%. Similarly, Gen-loaded niosomes reported in another study exhibited an EE of approximately 10% and failed to produce any significant enhancement in antibacterial activity based on MIC results.[81] Abdelghany et al[73] also reported Gen-loaded PLGA nanoparticles with EE values ranging from 6% to 22%, which exhibited higher MIC and MBC values than the pure drug against *Pseudomonas aeruginosa*. Other liposomal formulations have shown only moderate improvements in Gen antibacterial activity, primarily due to limited encapsulation efficiency and premature drug leakage[38] while PLGA nanoparticles have been constrained by low drug loading and rapid burst release.[39] In contrast, the polymer–lipid hybrid nanoparticles developed in this study achieved a substantially higher EE (42%) and a controlled-release profile, resulting in up to a 160-fold reduction in MIC and MBC values against resistant *S. aureus*. These findings underscore the distinct advantage of integrating a hydrophobic polymeric core with a lipid shell to enhance nanoparticle stability, modulate drug release, and overcome the encapsulation challenges typically associated with hydrophilic antibiotics such as Gen.

The superior antibacterial activity of F4 likely arises from the synergistic effects of its PLN composition. The lipid layer enhances adhesion and fusion with bacterial membranes, promoting drug entry into cells, while the polymeric matrix ensures prolonged release, thereby sustaining bactericidal levels even in the presence of efflux mechanisms. Previous reports have demonstrated that lipid-coated or hybrid nanoparticles significantly improve antibiotic penetration through biofilm matrices and reduce efflux-mediated clearance.[71,72] Thus, the structural design of F4 not only improves drug stability and retention but also enables effective circumvention of major bacterial resistance mechanisms. The observed differences in response between susceptible (E. coli ATCC-25922, MRSA-60, and EC-157) and resistant strains are consistent with expectations based on their intrinsic resistance profiles and validate the formulation's potential in overcoming antimicrobial resistance rather than enhancing activity against already-sensitive bacteria.

We acknowledge that the current work is limited to in vitro characterization and antibacterial assays, and that scalability and biocompatibility require further validation. We note that large-scale production of PLNs may require

optimization of solvent removal and homogenization parameters to ensure reproducibility. Additionally, cytotoxicity and in vivo pharmacokinetic studies are required to assess systemic safety, biodistribution, and therapeutic efficacy.

Conclusion

This study successfully developed and optimized a PLN nanoparticle system (F4) for the effective encapsulation and controlled release of Gen. The emulsification-solvent evaporation method was successfully modified to achieve high loading of Gen into PLN, addressing the significant challenge posed by the drug's extreme hydrophilicity. The optimized formulation exhibited favorable physicochemical characteristics, including nanoscale particle size, narrow size distribution, and high entrapment efficiency (42%), confirming its structural stability and suitability for antimicrobial delivery. Functionally, the F4 formulation demonstrated superior antibacterial efficacy compared with free Gen and previously reported Gen-loaded systems, achieving up to a 160-fold reduction in MIC and MBC values against resistant *Staphylococcus aureus*. The enhanced performance is attributed to the synergistic PLN architecture, which improves bacterial membrane interaction, and facilitates intracellular drug accumulation, thereby helping to overcome resistance mechanisms such as efflux pumps and biofilm penetration barriers. Comparative analysis with liposomal and PLGA-based nanocarriers highlighted the unique advantages of the F4 system in achieving higher drug encapsulation, greater stability, and higher antibacterial activity, overcoming the limitations of conventional hydrophilic antibiotic formulations. While the results are promising, future in vivo and cytotoxicity assessments are required to validate safety, scalability, and therapeutic performance. Overall, this study underscores the potential of PLN nanoparticles as a robust platform for the delivery of Gen, offering a promising strategy to enhance antibacterial efficacy and mitigate resistance in multidrug-resistant bacterial infections. Future studies will focus on evaluating the biocompatibility of the optimized PLNs through cytotoxicity assays on relevant mammalian cell lines and hemolysis testing. In vivo pharmacokinetic and histopathological analyses will further confirm their systemic safety and tissue compatibility.

Acknowledgments

The authors acknowledge the King Abdullah International Medical Research Center (KAIMRC), Ministry of National Guard-Health Affairs, for funding this work through Grant No. RC20/109/R and SP22R/226/10. The funding agency had no role in the study design, data collection, analysis, manuscript preparation, or the decision to publish.

Disclosure

This paper has been uploaded to preprints.org server as a preprint: https://www.preprints.org/frontend/manuscript/010c496e6f6d975923b7bca90d994714/download_pub.

The authors report no conflicts of interest in this work.

References

1. Antimicrobial Resistance Collaborators. Global burden of bacterial antimicrobial resistance in 2019: a systematic analysis. *Lancet*. 2022;399:629–655.
2. Prestinaci F, Pezzotti P, Pantosti A. Antimicrobial resistance: a global multifaceted phenomenon. *Pathog Glob Health*. 2015;109(7):309–318. doi:10.1179/2047773215Y.0000000030
3. Cassini A, Högberg L, Plachouras D, et al. Attributable deaths and disability-adjusted life-years caused by infections with antibiotic-resistant bacteria in the EU and the European Economic Area in 2015: a population-level modelling analysis. *Lancet Infect Dis*. 2019;19(1):56–66.
4. Centers for Disease Control and Prevention, US Department of Health and Human Services. Antibiotic Resistance Threats in the United States. Atlanta, GA: CDC; 2013. Available from: https://www.cdc.gov/antimicrobial-resistance/media/pdfs/ar-threats-2013-508.pdf. Accessed January 16, 2025.
5. Nwobodo DC, Ugwu MC, Anie CO, et al. Antibiotic resistance: the challenges and some emerging strategies for tackling a global menace. *J Clin Lab Anal*. 2022;36(9):e24655. doi:10.1002/jcla.24655
6. Nadgir CA, Biswas DA. Antibiotic resistance and its impact on disease management. *Cureus*. 2023;15(4):e38251. doi:10.7759/cureus.38251
7. Cepas V, López Y, Muñoz E, et al. Relationship between biofilm formation and antimicrobial resistance in Gram-negative bacteria. *Microb Drug Resist*. 2019;25(1):72–79.
8. Sharma S, Mohler J, Mahajan R, et al. Microbial biofilm: a review on formation, infection, antibiotic resistance, control measures, and innovative treatment. *Microorganisms*. 2023;11(6):1614. doi:10.3390/microorganisms11061614
9. Costerton JW, Geesey GG, Cheng KJ. How bacteria stick. *Sci Am*. 1978;238:86–95. doi:10.1038/scientificamerican0178-86

10. Costerton JW, Stewart PS, Greenberg EP. Bacterial biofilms: a common cause of persistent infections. *Science*. 1999;284:1318–1322. doi:10.1126/science.284.5418.1318
11. Høiby N, Ciofu O, Johansen HK, et al. The clinical impact of bacterial biofilms. *Int J Oral Sci*. 2011;3(2):55–65.
12. Michaelis C, Grohmann E. Horizontal gene transfer of antibiotic resistance genes in biofilms. *Antibiotics*. 2023;12(2):328. doi:10.3390/antibiotics12020328
13. Krause KM, Serio AW, Kane TR, et al. Aminoglycosides: an overview. *Cold Spring Harb Perspect Med*. 2016;6(6):a027029. doi:10.1101/cshperspect.a027029
14. Germovsek E, Barker CI, Sharland M. What do I need to know about aminoglycoside antibiotics? *Arch Dis Child Educ Pract Ed*. 2017;102(2):89–93.
15. Bernd B, Cooper MA. Aminoglycosides antibiotics in the 21st century. *ACS Chem Biol*. 2013;8(1):105–115. doi:10.1021/cb3005116
16. Xie J, Talaska AE, Schacht J. New developments in aminoglycoside therapy and ototoxicity. *Hear Res*. 2011;281(1–2):28–37. doi:10.1016/j.heares.2011.05.008
17. Streetman DS, Nafziger AN, Destache CJ, et al. Individualized pharmacokinetic monitoring results in less aminoglycoside-associated nephrotoxicity and fewer associated costs. *Pharmacotherapy*. 2001;21:443–451. doi:10.1592/phco.21.5.443.34490
18. Fausti SA, Frey RH, Henry JA, et al. Early detection of ototoxicity using high-frequency, tone burst-evoked auditory brainstem responses. *J Am Acad Audiol*. 1992;3:397–404.
19. Labby KJ, Garneau-Tsodikova S. Strategies to overcome the action of aminoglycoside-modifying enzymes for treating resistant bacterial infections. *Future Med Chem*. 2013;5(11):1285–1309. doi:10.4155/fmc.13.80
20. Wright GD. Molecular mechanisms of antibiotic resistance. *Chem Commun*. 2011;47(14):4055–4061. doi:10.1039/c0cc05111j
21. Miller GH, Sabatelli FJ, Hare RS, et al. The most frequent aminoglycoside resistance mechanisms—changes with time and geographic area: a reflection of aminoglycoside usage patterns? *Clin Infect Dis*. 1997;24(Suppl 1):S46–S62. doi:10.1093/clinids/24.supplement_1.s46
22. Biswas S, Raoult D, Rolain JM. A bioinformatic approach to understanding antibiotic resistance in intracellular bacteria through whole genome analysis. *Int J Antimicrob Agents*. 2008;32(3):207–220. doi:10.1016/j.ijantimicag.2008.03.017
23. Sabourian P, Yazdani G, Ashraf SS, et al. Effect of physico-chemical properties of nanoparticles on their intracellular uptake. *Int J Mol Sci*. 2020;21:8019. doi:10.3390/ijms21218019
24. Gelperina S, Kisich K, Iseman MD, Heifets L. The potential advantages of nanoparticle drug delivery systems in chemotherapy of tuberculosis. *Am J Respir Crit Care Med*. 2005;172(12):1487–1490. doi:10.1164/rccm.200504-613PP
25. Patra JK, Das G, Fraceto LF, et al. Nano based drug delivery systems: recent developments and future prospects. *J Nanobiotechnol*. 2018;16:71. doi:10.1186/s12951-018-0392-8
26. Yassin AEB, Albekairy A, Alkatheri A, Sharma RK. Anticancer-loaded solid lipid nanoparticles: high potential advancement in chemotherapy. *Dig J Nanomater Biostruct*. 2013;8(2):905–916.
27. Rajpoot K. Solid lipid nanoparticles: a promising nanomaterial in drug delivery. *Curr Pharm Des*. 2019;25(37):3943–3959.
28. Ghasemiyeh P, Mohammadi-Samani S. Solid lipid nanoparticles and nanostructured lipid carriers as novel drug delivery systems: applications, advantages and disadvantages. *Res Pharm Sci*. 2018;13(4):288–303. doi:10.4103/1735-5362.235156
29. Müller RH, Mäder K, Gohla S. Solid lipid nanoparticles (SLN) for controlled drug delivery – a review of the state of the art. *Eur J Pharm Biopharm*. 2000;50(1):161–177.
30. Aljihani SA, Alehaideb Z, Alarfaj RE, et al. Enhancing azithromycin antibacterial activity by encapsulation in liposomes/liposomal-N-acetylcysteine formulations against resistant clinical strains of Escherichia coli. *Saudi J Biol Sci*. 2020;27(11):3065–3071. doi:10.1016/j.sjbs.2020.09.012
31. Serpe L, Catalano MG, Cavalli R, et al. Cytotoxicity of anticancer drugs incorporated in solid lipid nanoparticles on HT-29 colorectal cancer cell line. *Eur J Pharm Biopharm*. 2004;58(3):673–680. doi:10.1016/j.ejpb.2004.03.026
32. Battaglia L, Serpe L, Muntoni E, et al. Methotrexate-loaded SLNs prepared by coacervation technique: in vitro cytotoxicity and in vivo pharmacokinetics and biodistribution. *Nanomedicine*. 2011;6(9):1561–1573. doi:10.2217/nnm.11.52
33. Lai P, Daear W, Löbenberg R, Prenner EJ. Overview of the preparation of organic polymeric nanoparticles for drug delivery based on gelatine, chitosan, poly(D,L-lactide-co-glycolic acid) and polyalkylcyanoacrylate. *Colloids Surf B Biointerfaces*. 2014;118:154–163. doi:10.1016/j.colsurfb.2014.03.017
34. El-Say KM, El-Sawy HS. Polymeric nanoparticles: promising platform for drug delivery. *Int J Pharm*. 2017;528:675–691. doi:10.1016/j.ijpharm.2017.06.052
35. Hallan SS, Kaur P, Kaur V, Mishra N, Vaidya B. Lipid polymer hybrid as emerging tool in nanocarriers for oral drug delivery. *Artif Cells Nanomed Biotechnol*. 2016;44(1):334–349. doi:10.3109/21691401.2014.951721
36. Sivadasan D, Sultan MH, Madkhali O, Almoshari Y, Thangavel N. Polymeric lipid hybrid nanoparticles (PLNs) as emerging drug delivery platform—a comprehensive review of their properties, preparation methods, and therapeutic applications. *Pharmaceutics*. 2021;13(8):1291. doi:10.3390/pharmaceutics13081291
37. Zhang L, Chan JM, Gu FX, et al. Self-assembled lipid-polymer hybrid nanoparticles: a robust drug delivery platform. *ACS Nano*. 2008;2(8):1696–1702.
38. Alhariri M, Majrashi MA, Bahkali AH, et al. Efficacy of neutral and negatively charged liposome-loaded gentamicin on planktonic bacteria and biofilm communities. *Int J Nanomed*. 2017;12:6949–6961.
39. Dhal C, Mishra R. In vitro and in vivo evaluation of gentamicin sulphate-loaded PLGA nanoparticle-based film for the treatment of surgical site infection. *Drug Deliv Transl Res*. 2020;10:1032–1043.
40. Razei A, Cheraghali AM, Saadati M, et al. Gentamicin-loaded chitosan nanoparticles improve its therapeutic effects on brucella-infected J774A.1 murine cells. *Galen Med J*. 2019;8:e1296.
41. Walker RJ, Keating GM. Aminoglycosides. In: Schwartz LB, Sutcliffe AI, editors. *Antibiotics: Discovery and Development*. New York, NY: Springer International Publishing; 2017:45–60.
42. Rao S, Prestidge CA. Polymer-lipid hybrid systems: merging the benefits of polymeric and lipid-based nanocarriers to improve oral drug delivery. *Expert Opin Drug Delivery*. 2016;13(5):691–707. doi:10.1517/17425247.2016.1151872

43. Jain S, Kumar M, Kumar P, et al. Lipid–polymer hybrid nanosystems: a rational fusion for advanced therapeutic delivery. *J Funct Biomater*. 2023;14(9):437. doi:10.3390/jfb14090437
44. Omer ME, Halwani M, Alenazi RM, et al. Novel self-assembled polycaprolactone–lipid hybrid nanoparticles enhance the antibacterial activity of ciprofloxacin. *SLAS Technol*. 2020;25(6):598–607. doi:10.1177/2472630320943126
45. CLSI. *M100-S27: Performance Standards for Antimicrobial Susceptibility Testing*. 27th ed. Wayne, PA: Clinical and Laboratory Standards Institute; 2017.
46. EUCAST/ESCMID. Determination of minimum inhibitory concentrations (MICs) of antibacterial agents by broth dilution. *Clin Microbiol Infect*. 2003;9:1–7.
47. Bolourchian N, Shafiee Panah M. The effect of surfactant type and concentration on physicochemical properties of carvedilol solid dispersions prepared by wet milling method. *Iran J Pharm Res*. 2022;21(1):e126913. doi:10.5812/ijpr-126913
48. Kitayama Y, Takigawa S, Harada A. Effect of poly(vinyl alcohol) concentration and chain length on polymer nanogel formation in aqueous dispersion polymerization. *Molecules*. 2023;28(8):3493. doi:10.3390/molecules28083493
49. Ekinci M, Yeğen G, Aksu B, Ilem-özdemir D. Preparation and evaluation of poly(lactic acid)/poly(vinyl alcohol) nanoparticles using the Quality by Design approach. *ACS Omega*. 2022;7(38):33793–33807. doi:10.1021/acsomega.2c02141
50. Cortés H, Hernández-Parra H, Bernal-Chávez SA, et al. Non-ionic surfactants for stabilization of polymeric nanoparticles for biomedical uses. *Materials*. 2021;14(12):3197. doi:10.3390/ma14123197
51. Masarudin MJ, Cutts SM, Evison BJ, et al. Factors determining the stability, size distribution, and cellular accumulation of small monodisperse chitosan nanoparticles as candidate vectors for anticancer drug delivery: application to the passive encapsulation of [^14C]-doxorubicin. *Nanotechnol Sci Appl*. 2015;8:67–80. doi:10.2147/NSA.S91785
52. Filipe V, Hawe A, Jiskoot W. Critical evaluation of nanoparticle tracking analysis (NTA) by NanoSight for measurement of nanoparticles and protein aggregates. *Pharm Res*. 2010;27(5):796–810. doi:10.1007/s11095-010-0073-2
53. Chatterjee S, Bhattacharya SK. Size-dependent catalytic activity of PVA-stabilized palladium nanoparticles in p-nitrophenol reduction: using a thermoresponsive nanoreactor. *ACS Omega*. 2021;6(32):20746–20757. doi:10.1021/acsomega.1c00896
54. Xiao-ting C, Wang T. Preparation and characterization of atrazine-loaded biodegradable PLGA nanospheres. *J Integr Agric*. 2019;18(5):1035–1041. doi:10.1016/S2095-3119(19)62613-4
55. Danaei M, Dehghankhold M, Ataei S, et al. Impact of particle size and polydispersity index on the clinical applications of lipidic nanocarrier systems. *Pharmaceutics*. 2018;10(2):57. doi:10.3390/pharmaceutics10020057
56. Chenthamara D, Subramaniam S, Ramakrishnan SG, et al. Therapeutic efficacy of nanoparticles and routes of administration. *Biomater Res*. 2019;23:20. doi:10.1186/s40824-019-0166-x
57. Hu Y, Yang Q, Kou J, Sun C, Li H. Aggregation mechanism of colloidal kaolinite in aqueous solutions with electrolyte and surfactants. *PLoS One*. 2020;15(9):e0238350. doi:10.1371/journal.pone.0238350
58. Rami ML, Meireles M, Cabane B, Guizard C. Colloidal stability for concentrated zirconia aqueous suspensions. *J Am Ceram Soc*. 2009;92:50–56. doi:10.1111/j.1551-2916.2008.02681.x
59. Musielak E, Feliczak-Guzik A, Nowak I. Optimization of the conditions of solid lipid nanoparticles (SLN) synthesis. *Molecules*. 2022;27(7):2202. doi:10.3390/molecules27072202
60. Pulingam T, Foroozandeh P, Chuah J-A, Sudesh K. Exploring various techniques for the chemical and biological synthesis of polymeric nanoparticles. *Nanomaterials*. 2022;12(3):576. doi:10.3390/nano12030576
61. Bohrey S, Chourasiya V, Pandey A. Polymeric nanoparticles containing diazepam: preparation, optimization, characterization, in vitro drug release and release kinetic study. *Nano Convergence*. 2016;3:3. doi:10.1186/s40580-016-0061-2
62. Alkholief M, Kalam MA, Anwer MK, et al. Effect of solvents, stabilizers and the concentration of stabilizers on the physical properties of poly(d, l-lactide-co-glycolide) nanoparticles: encapsulation, in vitro release of indomethacin and cytotoxicity against HepG2-cell. *Pharmaceutics*. 2022;14 (4):870. doi:10.3390/pharmaceutics14040870
63. Liu B, Dong Q, Wang M, et al. Preparation, characterization, and pharmacodynamics of exenatide-loaded poly(DL-lactic-co-glycolic acid) microspheres. *Chem Pharm Bull*. 2010;58(11):1474–1479. doi:10.1248/cpb.58.1474
64. Radwan MA. In vitro evaluation of polyisobutylcyanoacrylate nanoparticles as a controlled drug carrier for theophylline. *Drug Dev Ind Pharm*. 1995;21(20):2371–2375.
65. Gajbhiye KR, Salve R, Narwade M, et al. Lipid polymer hybrid nanoparticles: a custom-tailored next-generation approach for cancer therapeutics. *Mol Cancer*. 2023;22(1):160. doi:10.1186/s12943-023-01849-0
66. Sultan MH, Moni SS, Madkhali OA, et al. Characterization of cisplatin-loaded chitosan nanoparticles and rituximab-linked surfaces as target-specific injectable nano-formulations for combating cancer. *Sci Rep*. 2022;12(1):468. doi:10.1038/s41598-021-04427-w
67. Mehta M, Bui TA, Yang X, et al. Lipid-based nanoparticles for drug/gene delivery: an overview of the production techniques and difficulties encountered in their industrial development. *ACS Mater Au*. 2023;3(6):600–619. doi:10.1021/acsmaterialsau.3c00032
68. Kayan GÖ, Kayan A. Polycaprolactone composites/blends and their applications especially in water treatment. *Chem Engineering*. 2023;7(6):104. doi:10.3390/chemengineering7060104
69. Guo J, Pan Z, Fan L, et al. Effect of three different amino acids plus gentamicin against methicillin-resistant Staphylococcus aureus. *Infect Drug Resist*. 2023;16:4741–4754. doi:10.2147/IDR.S411658
70. Shi S, Lu W, Gu X, Lin Q. Efficacy of gentamicin-loaded chitosan nanoparticles against Staphylococcus aureus internalized in osteoblasts. *Microb Drug Resist*. 2024;30(5):196–202. doi:10.1089/mdr.2023.0066
71. Lee HW, Kharel S, Loo SCJ. Lipid-coated hybrid nanoparticles for enhanced bacterial biofilm penetration and antibiofilm efficacy. *ACS Omega*. 2022;7(40):35814–35824. doi:10.1021/acsomega.2c04662
72. Sadeghi Mohammadi S, Vaezi Z, Naderi-Manesh H. Improvement of anti-biofilm activities via co-delivery of curcumin and gentamicin in lipid-polymer hybrid nanoparticle. *J Biomater Sci Polym Ed*. 2021;33(2):174–196. doi:10.1080/09205063.2021.1982159
73. Abdelghany SM, Quinn DJ, Ingram RJ, et al. Gentamicin-loaded nanoparticles show improved antimicrobial effects towards Pseudomonas aeruginosa infection. *Int J Nanomed*. 2012;7:4053–4063. doi:10.2147/IJN.S34341
74. Abdel-Hakeem MA, Abdel Maksoud AI, Aladhadh MA, et al. Gentamicin-ascorbic acid encapsulated in chitosan nanoparticles improved in vitro antimicrobial activity and minimized cytotoxicity. *Antibiotics*. 2022;11(11):1530. doi:10.3390/antibiotics11111530

75. Ahangari A, Salouti M, Heidari Z, Kazemizadeh AR, Safari AA. Development of gentamicin-gold nanospheres for antimicrobial drug delivery to *Staphylococcal*-infected foci. *Drug Deliv.* 2013;20:34–39. doi:10.3109/10717544.2012.746406
76. Mohanta B, Chakraborty A, Selvara S, Roy A. Bactericidal effect of gentamicin conjugated gold nanoparticles. *Micro Nano Lett*. 2020;15:657–661. doi:10.1049/mna2.12007
77. Alzahrani RR, Alkhulaifi MM, Al Jeraisy M, et al. Enhancing gentamicin antibacterial activity by co-encapsulation with thymoquinone in liposomal formulation. *Pharmaceutics*. 2024;16(10):1330. doi:10.3390/pharmaceutics16101330
78. Maleki Dizaj S, Lotfipour F, Barzegar-Jalali M, Zarrintan MH, Adibkia K. Physicochemical characterization and antimicrobial evaluation of gentamicin-loaded $CaCO_3$ nanoparticles prepared via microemulsion method. *J Drug Deliv Sci Technol*. 2016;35:16–23. doi:10.1016/j.jddst.2016.05.004
79. Posadowska U, Brzychczy-Włoch M, Pamuła E. Gentamicin loaded PLGA nanoparticles as local drug delivery system for the osteomyelitis treatment. *Acta Bioeng Biomech*. 2015;17:41–48. doi:10.5277/ABB-00188-2014-02
80. Jia Y, Joly H, Omri A. Liposomes as a carrier for gentamicin delivery: development and evaluation of the physicochemical properties. *Int J Pharm*. 2008;359(1–2):254–263. doi:10.1016/j.ijpharm.2008.03.035
81. Forte J, Maurizi L, Fabiano MG, et al. Gentamicin loaded niosomes against intracellular uropathogenic Escherichia coli strains. *Sci Rep*. 2024;14:10196. doi:10.1038/s41598-024-59144-x

Nanotechnology, Science and Applications

Dovepress
Taylor & Francis Group

Publish your work in this journal

Nanotechnology, Science and Applications is an international, peer-reviewed, open access journal that focuses on the science of nanotechnology in a wide range of industrial and academic applications. It is characterized by the rapid reporting across all sectors, including engineering, optics, bio-medicine, cosmetics, textiles, resource sustainability and science. Applied research into nano-materials, particles, nano-structures and fabrication, diagnostics and analytics, drug delivery and toxicology constitute the primary direction of the journal. The manuscript management system is completely online and includes a very quick and fair peer-review system, which is all easy to use. Visit http://www.dovepress.com/testimonials.php to read real quotes from published authors.

Submit your manuscript here: https://www.dovepress.com/nanotechnology-science-and-applications-journal